doi:10.1093/brain/awr339 Brain 2012: 135; 447–460 | 447

BRAIN
A JOURNAL OF NEUROLOGY

Transplanted neural stem/precursor cells instruct phagocytes and reduce secondary tissue damage in the injured spinal cord

Melania Cusimano,[1] Daniela Biziato,[2,3] Elena Brambilla,[4] Matteo Donegà,[5] Clara Alfaro-Cervello,[5,6] Silvia Snider,[1] Giuliana Salani,[1] Ferdinando Pucci,[2,3] Giancarlo Comi,[3,7] Jose Manuel Garcia-Verdugo,[6] Michele De Palma,[2,*] Gianvito Martino[4,7] and Stefano Pluchino[1,5]

1 CNS Repair Unit, Institute of Experimental Neurology (InSpe), Division of Neuroscience, San Raffaele Scientific Institute, 20132 Milan, Italy
2 Angiogenesis and Tumour Targeting Unit and San Raffaele-Telethon Institute for Gene Therapy (HSR-TIGET), 20132 Milan, Italy
3 University Vita–Salute San Raffaele, 20132 Milan, Italy
4 Neuroimmunology Unit, InSpe, Division of Neuroscience, San Raffaele Scientific Institute, 20132 Milan, Italy
5 Department of Clinical Neurosciences, Cambridge Centre for Brain Repair and Cambridge Stem Cell Initiative, University of Cambridge, Cambridge CB2 0PY, UK
6 Unidad de Neurobiología Comparada, Instituto Cavanilles de Biodiversidad y Biología Evolutiva, University of Valencia, 46100, Spain
7 Department of Neurology and Neurophysiology and InSpe, San Raffaele Scientific Institute, 20132 Milan, Italy

*Present address: The Swiss Institute for Experimental Cancer Research (ISREC), Swiss Federal Institute of Technology Lausanne (EPFL), CH-1015, Lausanne, Switzerland

Correspondence to: Stefano Pluchino, MD, PhD,
Dept of Clinical Neurosciences,
Cambridge Centre for Brain Repair and Cambridge Stem Cell Initiative,
University of Cambridge,
E.D. Adrian Building, Forvie Site, Robinson Way,
Cambridge CB2 0PY, UK
E-mail: pluchino.stefano@hsr.it; spp24@cam.ac.uk

Transplanted neural stem/precursor cells possess peculiar therapeutic plasticity and can simultaneously instruct several therapeutic mechanisms in addition to cell replacement. Here, we interrogated the therapeutic plasticity of neural stem/precursor cells after their focal implantation in the severely contused spinal cord. We injected syngeneic neural stem/precursor cells at the proximal and distal ends of the contused mouse spinal cord and analysed locomotor functions and relevant secondary pathological events in the mice, cell fate of transplanted neural stem/precursor cells, and gene expression and inflammatory cell infiltration at the injured site. We used two different doses of neural stem/precursor cells and two treatment schedules, either subacute (7 days) or early chronic (21 days) neural stem/precursor cell transplantation after the induction of experimental thoracic severe spinal cord injury. Only the subacute transplant of neural stem/precursor cells enhanced the recovery of locomotor functions of mice with spinal cord injury. Transplanted neural stem/precursor cells survived undifferentiated at the level of the peri-lesion environment and established contacts with endogenous phagocytes via cellular–junctional coupling. This was associated with significant modulation of the expression levels of important inflammatory cell transcripts *in vivo*. Transplanted neural stem/precursor cells skewed the inflammatory cell infiltrate at the injured site by reducing the proportion of 'classically-activated' (M1-like) macrophages, while promoting the healing of the injured cord. We here identify a precise window of opportunity for the treatment of complex spinal cord injuries with therapeutically plastic somatic stem cells, and suggest

Received April 15, 2011. Revised October 17, 2011. Accepted October 30, 2011. Advance Access publication January 23, 2012

that neural stem/precursor cells have the ability to re-programme the local inflammatory cell microenvironment from a 'hostile' to an 'instructive' role, thus facilitating the healing or regeneration past the lesion.

Keywords: neural stem cells; spinal cord injury; cell transplantation; macrophages; immune regulation; tissue healing

Abbreviations: GFP = green fluorescent protein; NPC = neural precursor/stem cell; PBS = phosphate-buffered saline

Introduction

Several experimental regenerative therapies have been developed in the last few years with the aim(s) of reversing the devastating disability following spinal cord injuries (Schwab *et al*., 2006; Onose *et al*., 2009). At present, none of these approaches provides a full recovery in experimental injury models or humans (Moon and Bunge, 2005).

Recent advances in stem cell biology have raised the expectation that spinal cord injuries may be ameliorated by the delivery of variably potent stem cells (Barnabe-Heider and Frisen, 2008; Lindvall and Kokaia, 2010). However, extensive data are available showing that a limited degree of tissue repair and/or protection is achieved in preclinical models of spinal cord injury upon focal transplantation of stem cells, including somatic neural stem/precursor cells (NPCs) (Ogawa *et al*., 2002; Cummings *et al*., 2005; Karimi-Abdolrezaee *et al*., 2006). This is generally attributed to the limited numbers of transplanted NPCs that survive at the injury site and progress towards neuronal (Ogawa *et al*., 2002) or glial (Karimi-Abdolrezaee *et al*., 2006) differentiation, or both (Cummings *et al*., 2005). Intuitively, the combination of critically severe focal tissue damage—often affecting long projecting axons since the early phases after injury—and the limited capacity of transplanted neural stem cells to survive and integrate *in vivo* (Martino and Pluchino, 2006) together account for the limited therapeutic impact of NPC-based approaches in experimental spinal cord injury.

On the other hand, compelling evidence exists that systemic (e.g. intravenous) transplantation of NPCs ameliorates the clinicopathological features of chronic and relapsing experimental autoimmune encephalomyelitis, the animal model of multiple sclerosis (Pluchino *et al*., 2003, 2005), but also those of cerebral ischaemic stroke (Bacigaluppi *et al*., 2009), both in rodents and non-human primates (Aharonowiz *et al*., 2008; Pluchino *et al*., 2009*a*). We and others have shown that these latter effects are dependent on a number of multimodal neuroprotective and immune modulatory actions mediated by undifferentiated NPCs at perivascular sites *in vivo* (atypical ectopic niches) (Pluchino *et al*., 2005, 2009*a*, *b*). Yet, the detailed molecular and cellular mechanism(s) responsible for the multifaceted actions (therapeutic plasticity) exhibited by transplanted NPCs remain far from being fully elucidated, characterized and described.

We then asked to what extent, and how long after the lesion, therapeutically plastic NPCs exert their rescue and/or remodelling effects on the injured host environment (Pluchino *et al*., 2010); and whether these tissue remodelling effects may enhance functional recovery when NPCs are transplanted chronically to a severe spinal cord injury. To this aim, we adopted a preclinical approach seeking to investigate the cellular and molecular mechanisms sustaining the therapeutic plasticity of NPCs implanted focally at the peri-lesional site in mice suffering from subacute or early chronic severe experimental contusion spinal cord injury.

We adopted a complex mouse spinal cord injury model that displays the main anatomical, pathophysiological and behavioural features of complete spinal cord transection, inflicted an extremely severe (i.e. 2 N) thoracic contusion spinal cord injury; used two different NPC doses and two time-points of treatment (either subacute or early chronic to the injury); performed extensive assessment of locomotor functions, cell fate and interactions of transplanted NPCs with endogenous cells; and analysed gene expression, inflammatory cell infiltration and major pathological secondary events at the spinal cord injury site.

We found that subacute, but not early chronic, transplantation of NPCs led to significant recovery of locomotor functions, which became more evident when NPCs were transplanted in mice affected by a less severe (i.e. 0.75 N) contusion spinal cord injury model. Transplanted NPCs regulated the expression level of important inflammatory messenger RNA species at the level of the lesioned spinal cord segment, both in the subacute and early chronic treatment schedules. This was associated with undifferentiated NPCs establishing cell-to-cell contacts with endogenous phagocytes via cellular–junctional coupling, while surviving long-term next to blood vessels. NPC transplantation significantly reduced the proportion of 'classically-activated' (M1-like) macrophages (and increased that of regulatory T cells), while promoting the healing of the contused spinal cord.

In summary, our work identifies a precise window of opportunity for somatic stem cell-based approaches to treat complex spinal cord injuries and shows that NPC transplantation may work via reduction of the number of neurotoxic professional phagocytes *in situ*.

Our data further suggest that NPCs possess the functional promise of being able to 'correct' the local inflammatory environment from 'hostile' to 'instructive' for either the healing or the regeneration past the lesion (Pluchino *et al*., 2010).

Materials and methods

Neural stem/precursor cell derivation and cultures

Adult neurospheres were generated from the subventricular zone of 4- to 8-week-old C57Bl/6 mice, as described (Pluchino *et al*., 2003). Further details are provided in the Supplementary material.

Immunofluorescence

Details are provided in the Supplementary material.

Fluorescence-activated cell sorting analysis of neural stem/precursor cells *in vitro*

Fluorescence-activated cell sorting analysis for green fluorescent protein (GFP) and cell adhesion molecules on NPCs *in vitro* was performed as described (Pluchino *et al*., 2003). Further details are provided in the Supplementary material.

Contusion spinal cord injury

Mice were anaesthetized with ketamine/xylazine and a laminectomy was performed at the T12 vertebral level. M.C. and E.B. induced contusion spinal cord injury using a force of 2 N with an Infinite Horizons Impactor, (as described in Shechter *et al*., 2009) in a total of $n = 239$ 4- to 8-week-old (20–22 g) male C57Bl/6 mice (Charles River) ($n = 95$ for behavioural analyses; $n = 40$ for gene expression studies; $n = 84$ for *ex vivo* fluorescence-activated cell sorting analyses; and $n = 20$ for axonal tracing), as described elsewhere (Nishi *et al*., 2007). To induce a less severe contusion model, contusion spinal cord injury was induced using a force of 0.75 N with the Infinite Horizons Impactor on an additional $n = 40$ 4- to 8-week-old male C57Bl/6 mice. Postoperative care consisted of enrofloxacin (Baytril®, Bayer; 2.5 mg/kg, subcutaneously) once daily for 2 weeks. Urine was expelled by manual abdominal pressure twice daily for 1 week and then once daily for the duration of the experiment. Details on the study design are presented in Supplementary Fig. 1.

Neural stem/precursor cell transplantation

NPC transplants were performed at either 7 or 21 days after spinal cord injury, as described (Cummings *et al*., 2005). At the time of transplantation, a volume of ice-cold phosphate-buffered saline (PBS; without Ca^{2+} and Mg^{2+}) sufficient for a final concentration of 75×10^3 or 150×10^3/μl was added to the pellet and kept in ice prior to injection, as described elsewhere (Cummings *et al*., 2005). Briefly, the mice were anaesthetized as above and the laminectomy site was re-exposed. The volume to inject (250 nl/injection site) was measured with a 5 μl Hamilton syringe and then placed on a sterile surface. Each volume to inject was drawn up by capillarity in custom-made (40–50 μm) glass capillary connected to an insulin syringe and injections performed under a surgery microscope. Each mouse received a total of four injections of either farnesylated GFP $(fGFP)^+$ NPCs or equal volume of vehicle bilaterally from midline at both the anterior aspect of T13 and the posterior aspect of T11. Phosphate-buffered saline injection was used as control treatment. NPCs at sub-culturing passage number $\leqslant 20$ were used in all experiments. All procedures involving animals were performed according to the guidelines of the Animal Ethical Committee of the San Raffaele Scientific Institute (IACUC no. 346 to S.P.).

Axonal tracing and quantification

To trace the axons of the corticospinal tract, on either the day of the injury (0 days post-injury or at 14 days post-injury), mice were stereotaxically injected with biotin dextran amine (10 000 molecular weight; 10% solution; Molecular Probes) at the level of the sensorimotor cortex using a 5 μl Hamilton microsyringe. A total of $n = 2$ injections for each hemisphere (0.75 μl each) were made at 1.5 mm lateral to the midline, 1.5 mm anterior to bregma and 1 mm lateral, 0.5 mm posterior to bregma, and at a depth of 0.5 mm from the cortical surface. Healthy mice ($n = 3$) were used as controls. Biotin dextran amine-injected mice were sacrificed at 2 weeks after injection and processed for quantitative histopathology both at the level of the medullary pyramid rostral to the pyramidal decussation, as well as at T12. In all cases, a total of $n = 3$ consecutive 30-μm thick tissue sections per site were used for quantification of corticospinal tract fibres. Quantification of the spared corticospinal tract in mice with spinal cord injury was made on the normal appearing spinal cord 500 μm rostral to the epicentre of the lesion. For biotin dextran amine staining, floating sections were washed three times in PBS and 0.1% Triton X-100, incubated overnight with avidin and biotinylated horseradish peroxidase (Vectastain ABC Kit; Vector), washed again three times in PBS, and then reacted with 3,3′diaminobenzidene in 50 mM Tris buffer, pH 7.6, 0.024% hydrogen peroxide and 0.5% nickel chloride. Stained sections were mounted on microscope slides, preserving serial order. Electronic images were acquired with Leica DM 4000B microscope and the corticospinal tract area (mm^2) calculated using ImageJ software. To correct for inter-animal tracing variability the area of the labelled corticospinal tract at T12 was normalized in each mouse to the area of labelled corticospinal tract at the pyramidal decussation. Data were expressed as mean per cent of labelled corticospinal tract (±SEM) over healthy controls, slightly modified from Nielson *et al*. (2010).

Assessment of locomotor function

The recovery of open-field locomotor performance was evaluated by three investigators (M.D., S.S. and G.S.) blinded to surgery and treatment using the Basso Mouse Scale, as described (Shechter *et al*., 2009). Further details are provided in the Supplementary material.

Tissue processing and histopathology

At designated time points, mice were deeply anaesthetized with chloral hydrate 0.08 M and transcardially perfused with PBS and 4% paraformaldehyde. Spinal cords were removed and post-fixed in the same solution for 12 h at 4°C and then washed with PBS. The dissected spinal cords were cryoprotected for at least 24 h in 30% sucrose (Sigma) in PBS at 4°C, then the cords were embedded in Optimal Cutting Temperature (OCT) Tissue Tek compound (EM sciences) and snap frozen with liquid nitrogen. Frozen cord blocks were placed in a cryostat (Leica) and 10-μm thick axial sections were cut and collected onto SuperfrostPlus slides (Menzel-Glaser, Thermo Fisher Scientific) and processed for histopathology. A total of 7 mm of each cord segment (centred on the impact site) was cut, collected as $n = 10$ sets of serial sections (100 μm apart) and stored at −20°C. Four spinal cord segment-informative tissue slides (each containing $n = 18$ spinal cord 10-μm tick axial sections, for a total of $n = 72$ 10-μm thick axial cord sections per mouse) were processed for qualitative and quantitative histopathology and histochemistry. To determine the cell number and phenotype of *in vivo* transplanted NPCs, immunostainings for GFP (or direct fluorescence) and other markers were performed. Appropriate anti-rat, -mouse, -goat and -rabbit fluorophore (Alexafluor 488, 546; Molecular Probes) or biotin (Amersham biosciences) conjugated secondary antibodies were used. Nuclei were stained with 4′-6-diamidino-2-phenylindole (DAPI; Roche). The analysis of the NPC phenotype *in vivo* was performed by confocal microscopy (Leica DM 6000B) on 10-μm thick frozen tissue sections from mice with spinal

cord injury injected with either dosage of NPCs at both 7 and 21 days post-injury ($n = 2$–3 representative cord sections/mouse showing GFP immune reactivity; $n = 4$ mice/treatment group). A Leica M4000B microscope with motorized stage and Neurolucida (Version 8.0 Software, Microbrightfield) were used to stereologically calculate the volumes of the lesion, the volumes of demyelination, as well as the total cell numbers. Further details are provided in the Supplementary material.

Electron microscopy

Details are provided in the Supplementary material.

Gene expression analysis

The expression levels of messenger RNAs involved in inflammation, axonal growth, astrogliosis and remyelination were determined with a TaqMan® Array Microfluidic Card (96b format), at the level of the lesioned cord segment extending between T11 and T13 at 7, 14, 21 and 28 days post-injury, as described (Pluchino *et al*., 2008). Details are provided in the Supplementary material.

Ex vivo fluorescence-activated cell sorting analyses and cell sorting

Mice subjected to spinal cord injury were killed by an overdose of anaesthetic and their spinal cord processed for flow cytometry analysis by perfusion with PBS via the left ventricle. The lesioned cord segments extending between T11 and T13 were homogenized and reduced to single-cell suspensions by collagenase IV (2 mg/ml), dispase (0.2 mg/ml) and DNase I (0.1 mg/ml) treatment (30 minutes in Iscove's Modified Dulbecco's Medium containing 2% foetal bovine serum at 37°C). We positively selected total $CD45^+$ leucocytes by magnetic sorting (CD45 MicroBeads, Miltenyi). Cells were then incubated with 5% rat serum and 5 μg/ml rat anti-mouse Fcγ III/II receptor (CD16/CD32) blocking antibodies (BD PharMingen), and then stained using the monoclonal antibodies that are described in the Supplementary material.

We also sorted the following cell subsets: (i) $7AAD^-/CD45^+/F4/80^+/CD206$ $(MRC1)^{low/-}/CD11c^+$ cells (classically activated, M1-like macrophages); (ii) $7\text{-}AAD^-/CD45^+/F4/80^+/$ $CD206^{high}/CD11c^-$ cells (alternatively activated, M2-like macrophages); and (iii) $7AAD^-/CD45^+/F4/80^-/CD3^+$ cells (T cells).

All gates were set based on a specific fluorescence minus one (FMO) control. To sort cells, we used a MoFlo apparatus (Dako). After sorting, purity of the cells was always ⩾90%. Cellular sorting was performed on pools of $n = 8$–10 mice/treatment group, from a total of $n \geqslant 2$ independent experiments, leading to a total of 24–30 mice/treatment group. Total $1.2–35 \times 10^4$ cells were obtained from each independent cell sorting, and washed in low-protein buffer. Sorted cells from individual mice were pooled and then processed for RNA isolation, reverse transcription and real-time polymerase chain reaction, as described below. Further details are provided in the Supplementary material.

Neural stem/precursor cell microglia/macrophages co-cultures

The BV-2 cell line (gift from Dr Francesca Aloisi, Istituto Superiore di Sanità, Rome, Italy) cell line was cultured as described previously (Donnelly *et al*., 2011), and used for experiments at a passage number ⩽15. BV-2 cells were seeded at a density of 27×10^3 cells/cm^2 in culture medium only (resting) (Dulbecco's Modified Eagles Medium + 10% foetal bovine serum, 1% Penicillin/Streptomycin, 1% L-glutamine; all reagents from Invitrogen) or culture medium + lipopolysaccharide (100 ng/ml) (activated). After 2 h *in vitro*, two types of co-cultures with $fGFP^+$ NPCs were established as follows: (i) Mixed (same well) type: $fGFP^+$ NPCs were added directly to resting versus activated BV-2 cells at 1:10 and 1:2 ratios in T75 flasks. Six hours later, mixed type co-cultures were detached from the flask, and separation of GFP^- BV-2 cells from $fGFP^+$ NPCs performed by cell sorting using Dako Cytomation MoFlo FACS, as described (Engstrom *et al*., 2002). Fluorescence-activated cell sorted GFP^- BV-2 cells were collected in culture medium and processed for RNA isolation, reverse transcription and real-time polymerase chain reaction; and (ii) Insert (trans well) type: $fGFP^+$ NPCs (at 1:10 and 1:2 ratios) were seeded into cell culture inserts (0.4-μm pore size, Millipore) and then placed on the top of six-well plates containing resting versus activated BV-2 cells. Six hours later, inserts were removed; BV-2 cells detached, washed with PBS and processed for RNA isolation, reverse transcription and real-time polymerase chain reaction, as described below.

RNA isolation, reverse transcription and quantitative real-time polymerase chain reaction

Cells were lysed for total RNA extraction using the RNeasy® Micro kit (Qiagen) kit guidelines. RNA was retrotranscribed with SuperScript® III (VILO™ kit, Invitrogen). Quantitative polymerase chain reaction analyses were performed with TaqMan® probes from Applied Biosystems. Quantitative polymerase chain reactions were run for 40 cycles in standard mode using an ABI7900HT apparatus (Applied Biosystems). Further details are provided in the Supplementary material.

Statistical analysis

Data were analysed using a two-way repeated measures analysis of variance (ANOVA) followed by Bonferroni's *post hoc* test correction. Differences in gene expression were calculated by a Student's *t*-test.

Results

Functional recovery after subacute, but not early chronic, neural stem/precursor cell transplantation

We first tested the therapeutic potential of subacute (7 days post-injury) and early chronic (21 days post-injury) focal implantation of NPCs in the spinal cord of mice suffering from an extremely severe contusion spinal cord injury, which we caused by applying the impact force (i.e. 2 N) that is usually described for experimental severe spinal cord injury in rats (Beck *et al*., 2010). This severe injury led to minimal extent of spontaneous recovery of locomotor functions (Fig. 1A and B) and to major secondary events, including significantly high volumes of injury, demyelination and inflammatory cell infiltration, as well as a remarkable $48.1 \pm 5.6\%$ severance (i.e. retrograde 'die-back' degeneration) of the corticospinal tract quantified on spinal cord sections rostral

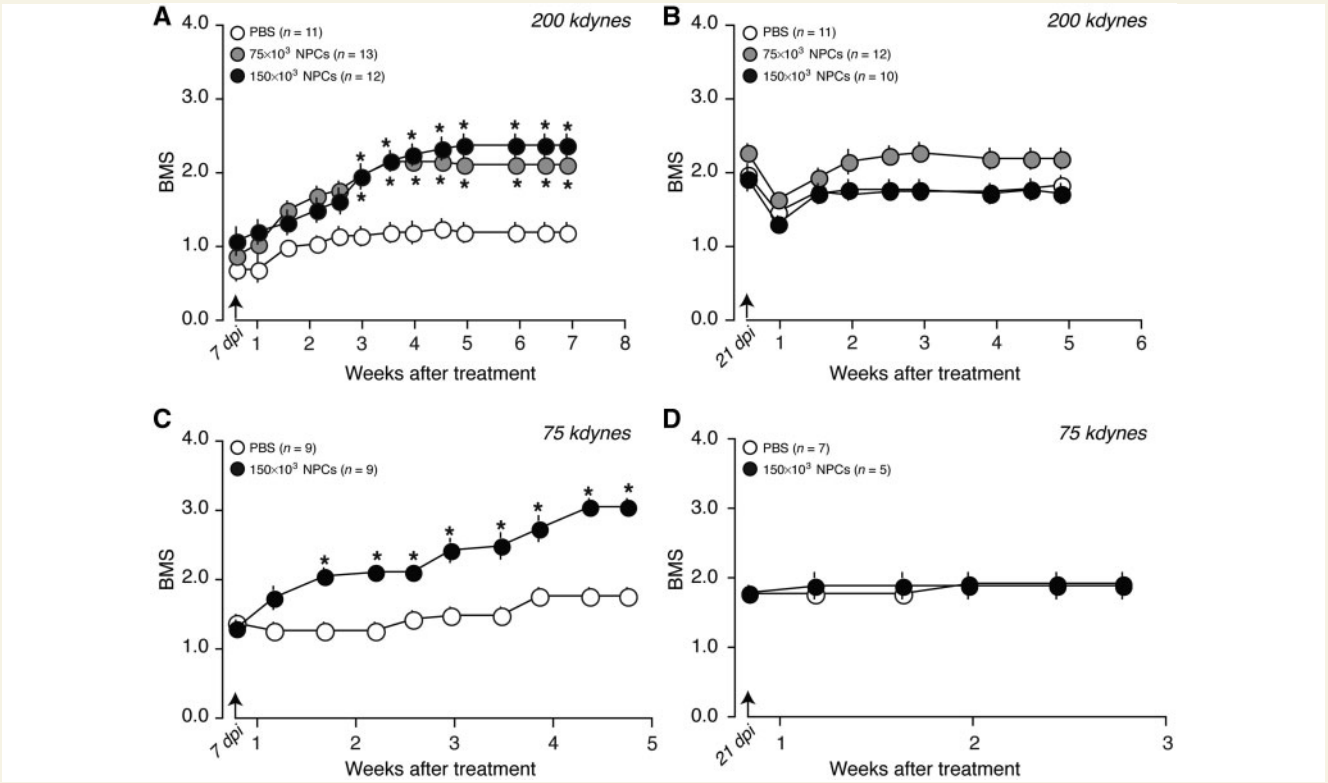

Figure 1 Recovery of locomotor functions after subacute, but not chronic, NPC transplantation in mice with contusion spinal cord injury. Amelioration of locomotor functions by subacutely (**A** and **C**), but not chronically (**B** and **D**) transplanted NPCs in mice suffering from spinal cord injuries. The arrow indicates the day of treatment. Data are mean Basso Mouse Scale (BMS ± SEM). $^*P \leqslant 0.001$, versus PBS-treated controls. dpi = days post-injury.

to the impact site at 21 days post-injury (Supplementary Fig. 2; $P \leqslant 0.01$, versus 7 days post-injury). This unusually severe spinal cord injury was reasonably well tolerated, as only 4.6% of mice (11/239) died within the first week after the injury (Supplementary Fig. 1).

NPCs were tagged *in vitro* with lentiviral vectors carrying either enhanced GFP or farnesylated GFP (Supplementary Fig. 3) (Follenzi *et al*., 2000). Both GFP and farnesylated GFP NPC lines retained very high levels of the typical NPC markers α4 integrin, CD44 and, to a much lower extent, the chemokine receptor CXCR4 (Supplementary Fig. 3) (Pluchino *et al*., 2005, 2009*a*, *b*). Hence, the NPCs used in this study expressed the surface molecules that are likely to be critical for sensing microenvironmental cues and for modulating regulatory cell behaviour after transplantation (Pluchino *et al*., 2005). Transplantation experiments were performed using two different dosages of farnesylated GFP-transduced NPCs (Supplementary Fig. 3) and included PBS-injected mice with spinal cord injury as controls.

We observed that subacute, but not early chronic focal NPC transplantation led to significant recovery of locomotor functions, which started at 2 weeks after transplantation and was measurable up to the end of the follow-up (7 weeks after transplantation), compared with PBS-treated controls. We did not observe any difference in the therapeutic impact of 75×10^3 versus 150×10^3 NPCs (Fig. 1A and B). The observed recovery of locomotor functions became even more evident when NPC transplantation was applied to a less severe (e.g. 0.75 N) contusion spinal cord injury model (Fig. 1C). Also in this latter spinal cord injury model, the early chronic focal NPC transplantation failed to evoke any behavioural changes (Fig. 1D).

Promotion of healing in the injured spinal cord

We then sought to investigate the effects of the subacute versus early chronic transplantation of NPCs on major secondary events occurring after the spinal cord injuries, such as the volume of the injury, the volume of demyelination in the spared tissue, and the extent of inflammatory cell infiltration. All the anatomical analyses related to the NPC transplantation were carried out only in mice receiving 2 N injuries.

Quantification of tissue injury at 1 week after treatment did not reveal any significant difference between NPC- and PBS-treated mice with spinal cord injury (Supplementary Fig. 4). On the other hand, we observed a significant reduction of the volumes of injury and demyelination in mice with spinal cord injury subacutely transplanted with NPCs versus PBS-treated controls (Fig. 2A and B). At 7 weeks after NPC transplantation, we also observed a trend towards reduction of the Iba1$^+$ macrophage/microglial infiltration at the injury site in mice with spinal

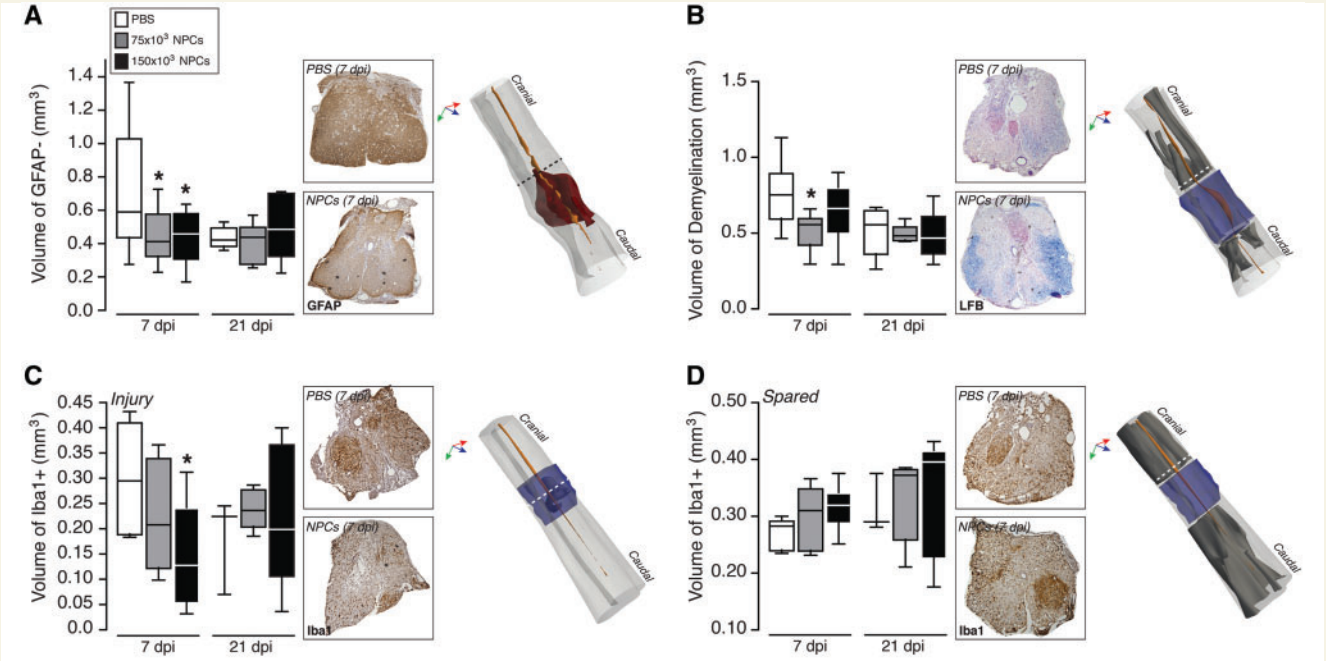

Figure 2 Promotion of healing in the severely injured spinal cord. (**A–D**) Stereological quantification of volumes of GFAP$^+$ tissue injury (**A**; red solid), Luxol fast blue (LFB)$^-$ demyelination (**B**; grey solid) and Iba1 +, at the level of the injured (grey solid in **C**) or spared (grey solid in **D**) cord tissue. In the 3D renderings, the solid orange in **A–D** is the central canal, while the solid transparent blue in **B–D** is the injury volume. Shown in **A–D** are also representative axial images of the stainings for stereological quantifications. Images have been taken at either 600 μm above the lesion (**A**, **B** and **D**) or at the lesion epicentre (**C**), as indicated by the dashed lines. Volumes in **A–D** have been calculated at 56 days after the injury. Data are minimum to maximum volumes from $n \geqslant 3$ mice per group. $^*P \leqslant 0.05$, versus PBS-treated controls. dpi = days post-injury; GFAP = glial fibrillary acidic protein.

cord injury subacutely transplanted with low-dose NPCs versus PBS-treated controls. This reached a statistical significance in high-dose NPC transplants (Fig. 2C). We did not observe any significant differences of Iba1$^+$ cell infiltration at the level of the spared cord at any cell dosage in any of the treatment groups (Fig. 2D).

Cellular–junctional coupling between transplanted undifferentiated neural stem/precursor cells and endogenous phagocytes

We then investigated the survival, integration and/or differentiation of transplanted NPCs *in vivo*. We first observed that 4–5.5% of transplanted GFP$^+$ NPCs showed a widespread distribution all over the analysed segment of the cord, including the lesion epicentre (Fig. 3A and B), at 1 week after transplantation (150×10^3 NPCs 7 days post-injury: 8171 ± 2216 GFP$^+$ cells; 150×10^3 NPCs at 21 days post-injury: 6038 ± 725 GFP$^+$ cells). At 7 weeks after transplantation, only 0.5–1% of transplanted NPCs survived in the spinal cord (150×10^3 NPCs 7 days post-injury: 643.5 ± 133.2 GFP$^+$ cells; 150×10^3 NPCs at 21 days post-injury: 931.8 ± 489.5 GFP$^+$ cells; both $P \leqslant 0.05$, versus 1 week after transplantation). In all cases, most NPCs accumulated outside the injured area (Fig. 3A, C and Supplementary Fig. 5), appeared organized at the boundaries of the injured tissue, in very close proximity to Iba1$^+$ cells and blood vessels (Fig. 3D). The confocal microscopy analysis of the cell-to-cell interactions at the level of these perivascular areas (niches) revealed the presence of tight contacts, up to structural junctional coupling, between GFP$^+$ NPCs and F4/80$^+$ macrophages (Fig. 3E and F), but not B220$^+$ putative B lymphocytes (Fig. 3G), that were established via connexin43$^+$. Phenotypically, none of the GFP$^+$ NPCs at the boundaries of the injured spinal cord expressed the neuronal marker NeuN, whereas between 11.5% (±3.7) and 15.1% (±1.7) of them stained for the astroglial lineage marker glial fibrillary acidic protein (GFAP). The helix–loop–helix transcription factor Olig2 was expressed by 3.1% (±1.5) and 14.1% (±5.2) of the GFP$^+$ NPCs when transplanted at either 7 or 21 days post-injury, respectively.

We performed pre-embedding immunogold staining for GFP and examined the extent of integration, morphology/ultrastructure and types of cell-to-cell interactions of transplanted NPCs using a transmission electron microscope. Immunogold-labelled transplanted NPCs surviving up to 7 weeks after transplantation were observed in small clusters through the host tissue. NPCs were systematically found outside the lesion site and were organized at the boundaries of the injury site and in very close proximity to blood vessels (Fig. 4A and B). We observed an extremely branched NPC morphology, with long processes running between endogenous cells (Fig. 4B). Large clusters of phagocytic cells accumulated next to the injury site, where NPCs were also found (Fig. 4A–C and Supplementary Fig. 6). Phagocytes were identified by their small irregular nucleus with clumped

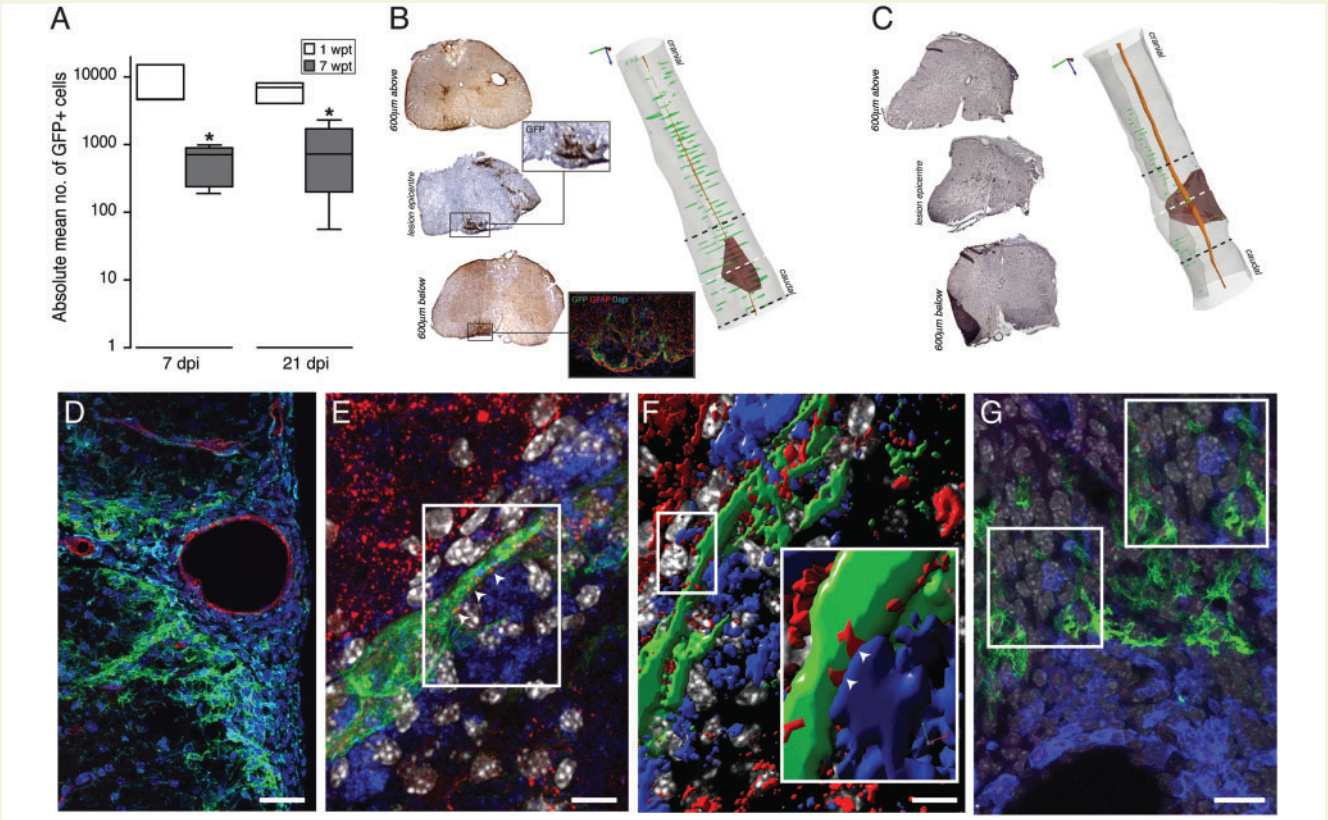

Figure 3 *In vivo* survival and integration transplanted NPCs. (**A**) Quantification of transplanted fGFP$^+$ NPCs *in vivo* at either 1 or 7 weeks post transplantation (wpt) of 150 $\times$ 10^3 NPCs. Data are absolute minimum to maximum numbers of fGFP$^+$ cells/mouse from $n \geqslant 3$ mice/group. *$P \leqslant 0.05$, as compared with 1 week after transplantation. (**B** and **C**) Representative axial images of the GFP staining (brown) for stereological quantifications in **A** from two representative mice with spinal cord injury sacrificed at 1 (**B**) or 7 (**C**) weeks after NPC transplantation. Haematoxylin staining in **B** and **D** is shown in blue. The fluorescent image in **B** shows detail of GFP$^+$ cells at the level of the perivascular area. In the 3D renderings, the red solid is GFAP, the green dots are GFP and the solid orange is the central canal. Dashed lines refer to representative axial images. (**D**) Confocal microscopy image of an 'atypical perivascular niche', where GFP$^+$ NPCs are found in very close vicinity to Iba1$^+$ cells (light blue). CD31$^+$ endothelial cells are in red. (**E**) Confocal microscopy image of GFP (green) NPCs contacting F4/80$^+$ macrophages via connexin43$^+$ cellular junctions (red; arrowheads). (**F**) Volocity®-based 3D reconstruction (from a total of $n = 20$ *Z*-stacks of optical slices in 0.3 µm intervals) of the confocal *Z*-stack in **E**. The magnified inset shows structural junctional connexin43 pattern (red; arrowheads) between the process of one NPC (green) and one juxtaposed F4/80$^+$ macrophage (blue). (**G**) Confocal microscopy image of GFP (green) NPCs and B220$^+$ putative B lymphocytes (blue) not establishing connexin43$^+$ (red) mediated junctional coupling in a perivascular spinal cord area. DAPI is blue in **D** and grey in **E–G**. Scale bars: **D** = 60 µm; **E** and **F** = 15 µm; **G** = 30 µm.

chromatin, a cytoplasm rich in short rough endoplasmic reticulum cisterns, abundant mitochondria and a heterogeneous variety of lysosomes/vacuoles (Supplementary Fig. 6). NPCs within perivascular niches displayed morphological features of immature cells (Fig. 4 A–C and Supplementary Fig. 6), showed an extremely interdigitated surface surrounded by basal lamina (Fig. 4F) and established regular cell contacts up to cellular junctions with both endogenous (i.e. immunogold-negative) phagocytes (Fig. 4A–C) and astrocytes (Fig. 4C–E).

Regulation of inflammatory messenger RNAs at the level of the injured spinal cord segment

To investigate the mechanisms regulating the clinicopathological recovery observed in spite of the low numbers of surviving NPCs, we performed a wide TaqMan® Low-Density Array (TLDA)-based gene expression profiling of the T11–T13 spinal cord segment of mice with spinal cord injury transplanted with NPCs at either 7 or 21 days post-injury, both these treatment groups being profiled at 1 week after NPC transplantation (the two time-points being profiled are hereafter referred to as 14 and 28 days post-injury, respectively). We profiled the expression levels of a total of 94 different messenger RNAs involved in: axonal growth (31/94; 32.9%), astrogliosis (20/94; 21.2%), inflammation (30/94; 31.9%) and myelination (14/94; 14.8%) (Supplementary material).

We observed significant impact of NPC transplantation on gene expression after subacute [22/94 genes (23.4%) with a $P \leqslant 0.05$] and, even more strikingly, chronic [38/94 genes (40.4%) with a $P \leqslant 0.05$], NPC transplantation (versus PBS-treated controls) (Fig. 5 and Supplementary Table 1).

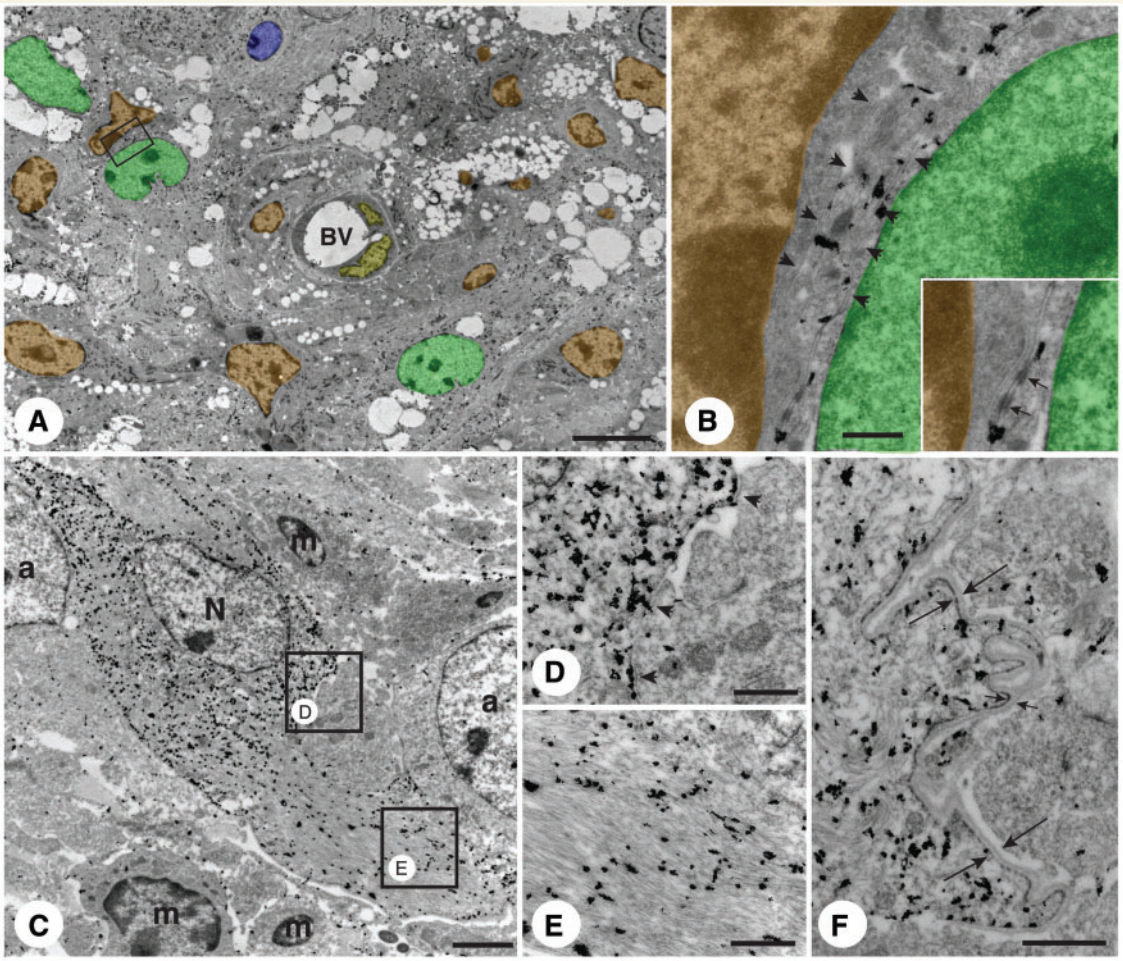

Figure 4 Morphology and ultrastructure of atypical perivascular NPC niches. (**A**) Electron micrograph of NPCs labelled with pre-embedding immunogold for GFP. NPCs are highly branched and accumulate at the level of perivascular niches. The main cellular components of these perivascular niches are infiltrating monocyte/macrophages that are identified by their scarce cytoplasm and irregular nucleus with clumped chromatin. The frame indicates one NPC whose processes are found in very close contact to a monocyte/macrophage. (**B**) High magnification of the frame in **A** showing the immunogold-labelled process of an NPC (arrowheads) running between a monocyte/macrophage and a second immunogold-labelled NPC. Cellular junctions between both NPC cytoplasms (inset, arrows) and between the NPC and the monocyte/macrophage can be observed in the inset. Pseudo colours in **A** and **B**: NPCs = green; monocytes/macrophages = orange; endothelial cells = yellow; endogenous astrocytes = blue. (**C**) Immunogold-labelled NPC (N) surrounded by two endogenous (immunogold-negative) astrocytes (a), and next to three infiltrating monocytes/macrophages (m). The two frames indicate sites of cell-to-cell contacts. (**D**) Detail of the contact between the NPC and one endogenous astrocyte (arrowheads). (**E**) Detail of cytoplasm of the NPC typically rich in intermediate filaments. (**F**) Detail of an immunogold-positive NPC showing an extremely interdigitated surface surrounded by basal lamina (between arrows). Images in **A–F** were collected at 50 days after transplantation. Scale bars: **A** = 5 μm; **B** = 200 nm; **C** = 2 μm; **D** and **E** = 500 nm; **F** = 1 μm. BV = blood vessel.

All the messenger RNAs that were significantly upregulated in the spinal cord of mice with spinal cord injury transplanted subacutely with NPCs were inflammatory genes. Among those showing higher fold induction, the chemokine *Ccl2* (11.15-fold; $P \leqslant 0.0001$), the cell adhesion molecules L-selectin (*Sell,* 2.8-fold; $P \leqslant 0.05$), lymphocyte function-associated antigen-1 (*Itgb2*, 4.95-fold; $P \leqslant 0.005$), vascular cell adhesion molecule-1 (*Vcam1*, 2.09-fold; $P \leqslant 0.005$), and intercellular cell adhesion molecule-1 (*Icam1*, 3.39-fold; $P \leqslant 0.005$), inducible nitric oxide synthase (*Nos2,* 4.06-fold; $P \leqslant 0.005$), and the suppressor of cytokine signalling-3 (*Asb3*, 2.35-fold; $P \leqslant 0.05$), were similarly upregulated in mice with spinal cord injury transplanted either subacutely or chronically with NPCs (Fig. 5 and Supplementary Table 1). On the other hand, the transplantation of NPCs downregulated the chemokine *Ccl3* (2.4-fold; $P \leqslant 0.005$), chondroitin sulphate proteoglycan-4 *(Cspg4)* (2.64-fold; $P \leqslant 0.005$) and ciliary neurotrophic factor *(Cntf)* (2.64-fold; $P \leqslant 0.005$). These messenger RNAs were found similarly downregulated at both 14 and 28 days post-injury (Fig. 5 and Supplementary Table 1).

The PBS treatment alone also induced significant upregulation of *Casp3* (1.81-fold; $P \leqslant 0.05$) and *Casp 8* (1.98-fold; $P \leqslant 0.01$), *H2k1 (*a MHC-I molecule*)* (1.88-fold; $P \leqslant 0.005$), and *Mmp2* (3.23-fold; $P \leqslant 0.01$), as well as some major regulators of astrogliosis, including versican (*Vcan*, 2.03-fold; $P \leqslant 0.0005$), neurocan

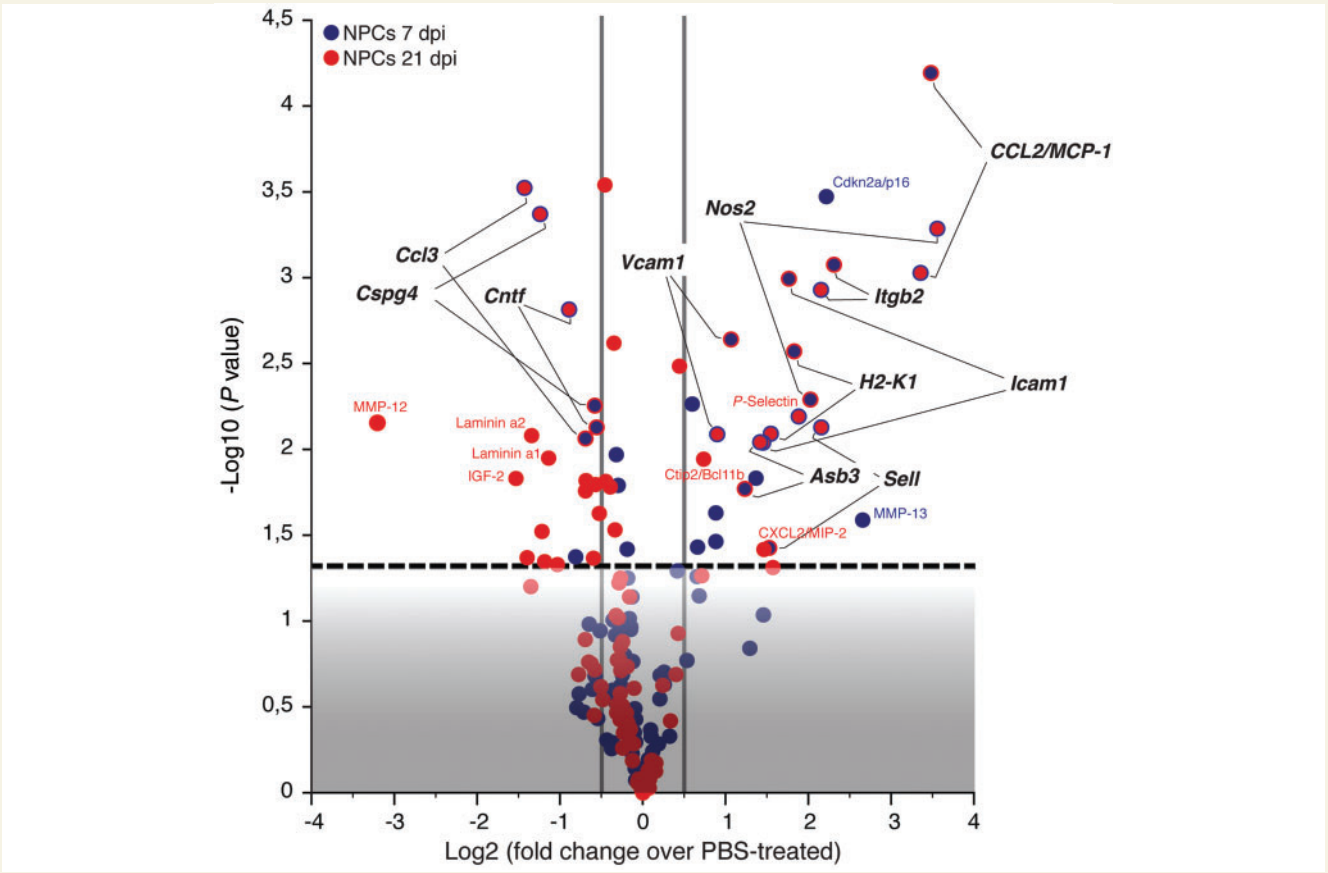

Figure 5 Modulation of gene expression. Volcano plot [x-axis = $\log_2$ (fold change); y-axis = $-\text{Log}_{10}$ (P-value)] showing statistically significant differentially expressed genes between mice with spinal cord injury transplanted at either 7 days post-injury or 21 days post-injury with 150×10^3 NPCs, as compared with mice with spinal cord injury injected with PBS at the same time points. Vertical grey lines ($x = -0.5$ and $x = 0.5$) correspond to fold changes of 0.7 and 1.4, respectively. The horizontal dashed line ($y = 1.3$) corresponds to a P-value = 0.05. Data have been calculated from $n = 5$ individual mice per treatment group.

(*Ncan*, 1.48-fold; $P \leqslant 0.05$) and *Cspg4* (1.61-fold; $P \leqslant 0.005$). These messenger RNAs were subjected to significant regulation only when the PBS treatment was applied chronically to the injury, as compared with untreated mice with spinal cord injury (Supplementary Fig. 7 and Supplementary Table 1).

Instruction of professional phagocytes towards a tissue-healing mode

To investigate the functional effects of the observed NPC-driven regulation of inflammatory messenger RNAs *in vivo*, we analysed the identity and phenotype of the inflammatory cells found on their neighbourhoods at the injury site. We performed seven-colour flow cytometry analysis of the CD45$^+$ cells isolated from the contused spinal cord segment 1 week after subacute NPC transplantation, and paid particular attention to the characterization of those subsets of inflammatory cells—including myeloid cells, but also T and B lymphocytes—with the potential to regulate post-traumatic pain, repair and/or regeneration, as well as functional recovery (Kigerl *et al*., 2009; Nucera *et al*., 2011).

Approximately 65–80% of all CD45$^+$ leukocytes isolated from the contused spinal cord segment were CD11b$^+$ myeloid cells in either group of mice (Fig. 6A). Of these, a sizable proportion were F4/80$^+$ macrophage-lineage cells (Beck *et al*., 2010) (Fig. 6B). Mice transplanted with NPCs contained smaller proportions of myeloid cells (Fig. 6A, $P \leqslant 0.005$) and macrophage-lineage cells (Fig. 6B; $P \leqslant 0.005$), compared with PBS-treated controls. Among the macrophage-lineage cells, the relative proportion of CD11c$^+$/CD206$^-$ inflammatory (M1-like) macrophages (Pucci *et al*., 2009) showed a highly significant 4.8-fold reduction in NPC-transplanted spinal cord injury mice (Fig. 6C; $P \leqslant 0.0001$, versus PBS treated). On the other hand, we did not observe a statistically significant change of the relative proportion of CD206$^+$/CD11c$^-$ tissue-remodelling/pro-angiogenic (M2-like) macrophages (Pucci *et al*., 2009) in the two treatment groups (Fig. 6D). NPC-transplanted mice with spinal cord injury also showed a significantly lower proportion of F4/80$^-$/CD11c$^+$ dendritic cells (Fig. 6E; $P \leqslant 0.005$, versus PBS-treated).

We also investigated the gene expression signature of the M1- and M2-like macrophages that were isolated from the spinal cord of PBS-treated mice. This was highly reminiscent of their tumour-derived counterpart (Pucci *et al*., 2009), with CD206$^+$/CD11c$^-$ (M2-like) macrophages showing significantly increased expression of *CD163* and *Lyve1* ($P \leqslant 0.005$ and $P \leqslant 0.05$, respectively) and

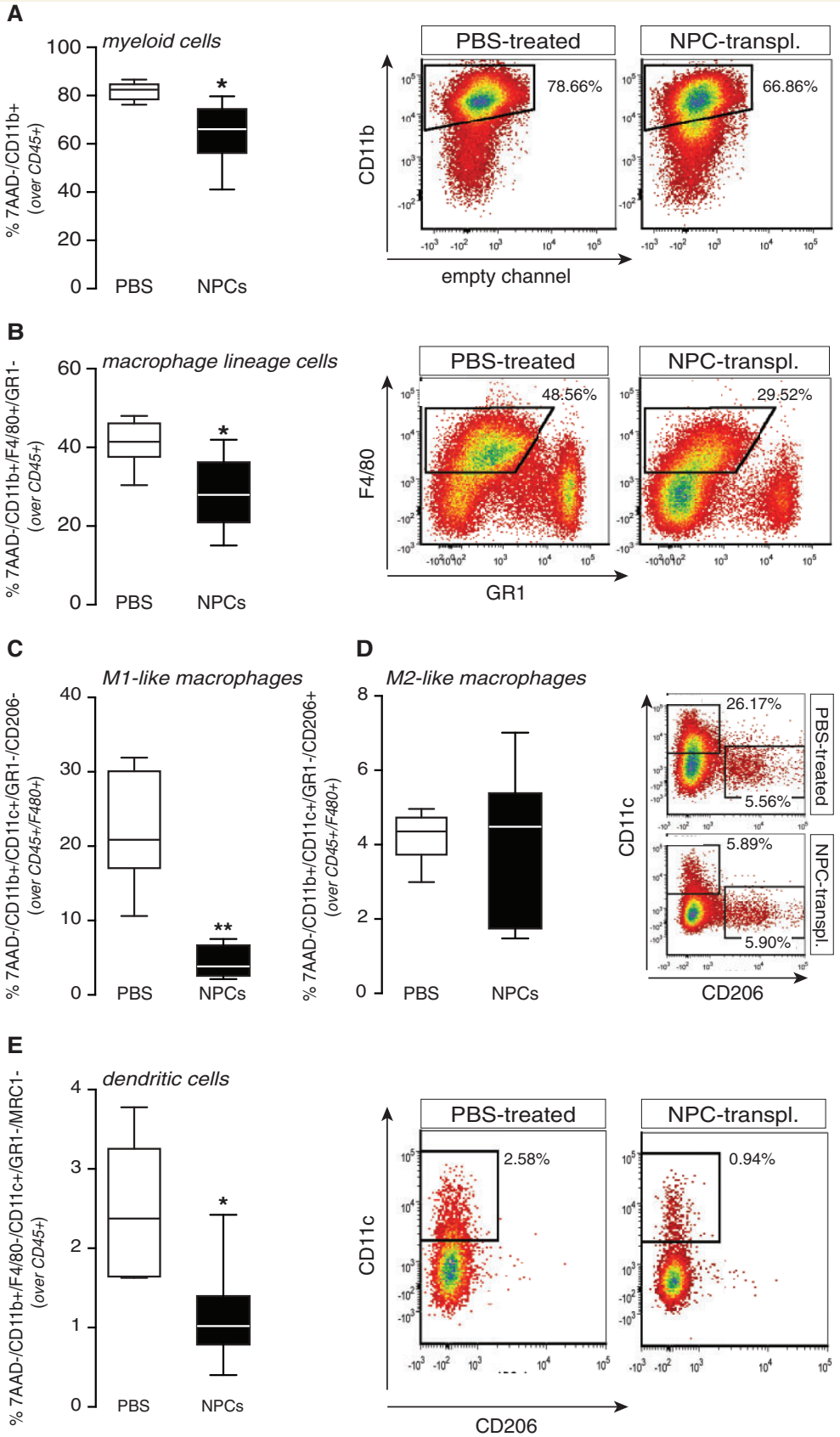

Figure 6 Instruction of professional phagocytes towards a tissue-healing mode. Flow cytometry analysis of myeloid cell subsets in the injured spinal cord at 14 days post-injury (7 days after subacute treatment). $CD45^+$ hematopoietic cells isolated from injured spinal cord were stained with 7-AAD to exclude non-viable cells from further analysis. (**A**) Myeloid cells; (**B**) macrophage lineage cells;

(continued)

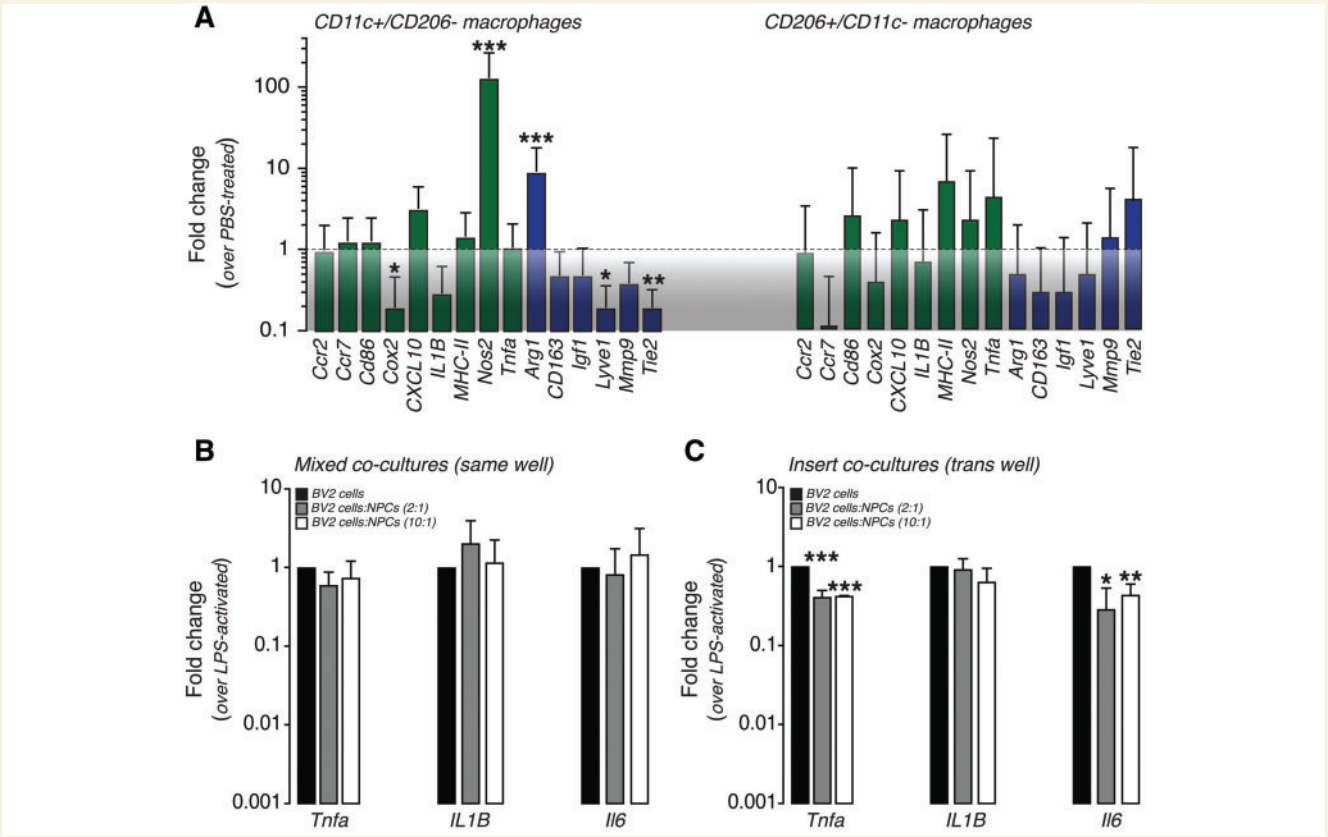

Figure 7 NPCs affect the gene signature of inflammatory professional phagocytes both *in vivo* and *in vitro*. (**A**) Gene signature of spinal cord injury-infiltrating macrophages in NPC-transplanted mice at 14 days post-injury (7 days after subacute treatment). Green bars are markers of M1-like macrophages, whereas blue bars are markers of M2-like macrophages. Data are mean fold changes (over PBS-treated) (± SEM) from $n = 24$–30 mice/treatment group and $n \geqslant 2$ independent experiments. (**B** and **C**) Expression of inflammatory messenger RNAs in BV-2 cells co-cultured with NPCs. Data are mean fold changes (over lipopolysaccharide-activated) (± SEM). $^{*}P \leqslant 0.05$; $^{**}P \leqslant 0.005$ and $^{***}P \leqslant 0.0001$. LPS = lipopolysaccharide.

a trend towards upregulation of *Arg1*, *Igf1* and *Tie2*, compared with $CD11c^{+}/CD206^{-}$ (M1-like) macrophages (Supplementary Fig. 8). At variance with $CD206^{+}$ tumour macrophages (Pucci *et al.*, 2009), $CD206^{+}/CD11c^{-}$ spinal cord injury macrophages displayed highly increased expression of *Nos2* ($P \leqslant 0.05$, versus $CD11c^{+}/CD206^{-}$ macrophages; Supplementary Fig. 8).

The NPC transplantation not only significantly reduced infiltration by $CD11c^{+}/CD206^{-}$ (M1-like) macrophages, but also had profound effects on their gene expression profile, which showed significant upregulation of both *Nos2* and *Arg1* (both $P \leqslant 0.0001$, versus PBS treated; Fig. 7A), and downregulation of *Cox2*, *Lyve1* (both $P \leqslant 0.05$, versus PBS treated) and *Tie2* ($P \leqslant 0.005$, versus PBS-treated; Fig. 7A). On the other hand, we did not observe any effects on the gene signature of $CD206^{+}/CD11c^{-}$ macrophages isolated from NPC-treated spinal cord injury mice, versus PBS-treated controls (Fig. 7A).

We also analysed $CD19^{-}/CD3^{+}$ T lymphocytes and $CD19^{+}/CD3^{-}$ B lymphocytes. Both these cells represented a minor haematopoietic cell infiltrate in the injured cord segment. Nonetheless, we noted a slight increase of the proportion of T lymphocytes (Supplementary Fig. 9; $P \leqslant 0.05$) and a significant reduction of B lymphocytes (Supplementary Fig. 9; $P \leqslant 0.005$) in NPC-transplanted versus PBS-treated controls. These data were also confirmed *in vivo* (Supplementary Fig. 9). The gene expression profile of the T lymphocytes isolated from the spinal cord of NPC-treated spinal cord injury mice showed significantly increased expression of the regulatory T-cell markers *CD25* and *Foxp3* ($P \leqslant 0.05$ and $P \leqslant 0.005$, versus PBS-treated), but also of the effector/cytotoxic

Figure 6 Continued
(**C**) 'classically-activated' (M1-like) inflammatory macrophages; (**D**) 'alternatively-activated' (M2-like) tissue-remodelling/pro-angiogenic macrophages; and (**E**) dendritic cells. All gates were set based on specific fluorescence minus one (FMO) control samples. For each myeloid cell subset, quantitative data are shown on the left, while representative density plots are shown on the right. White whiskers are mice with spinal cord injury injected with PBS, while black whiskers are spinal cord injury mice injected with 150×10^{3} NPCs. Data are minimum to maximum per cent of marker-positive cells from $n = 24$ mice/treatment group and a total of $n = 2$ independent experiments.
$^{*}P \leqslant 0.005$ and $^{**}P \leqslant 0.0001$, versus PBS-treated controls.

markers *CD8* ($P \leqslant 0.05$, versus PBS-treated), *Fasl*, *Gzmb* and *Ifng* (all $P \leqslant 0.0001$, versus PBS-treated) (Supplementary Fig. 8).

Finally, *in vitro* experiments with BV-2 cells confirmed the capacity of NPCs to interfere with the responsiveness of CNS phagocytes to canonical inflammatory stimuli (e.g. lipopolysaccharide) (Hoffmann *et al*., 1999)—likely via secreted products—as suggested by the significant decrease of *Tnfa* ($P \leqslant 0.0001$, versus lipopolysaccharide-activated) and *Il6* ($P \leqslant 0.05$, versus lipopolysaccharide-activated) in 'insert' (trans well), but not in 'mixed' (same well) co-cultures (Fig. 7B and C).

Discussion

Compelling evidence exists that transplanted NPCs possess a remarkable ability to mediate efficient bystander myelin repair and axonal protection/rescue in immune-mediated experimental CNS demyelination and stroke (Pluchino *et al*., 2005, 2009*a*, *b*; Bacigaluppi *et al*., 2009; Einstein *et al*., 2009). The evidence for the functional potency of NPCs is complemented by parallel data demonstrating their capacity to differentiate into multiple neural lineages upon transplantation in neurological disease models (Ogawa *et al*., 2002; Cummings *et al*., 2005; Karimi-Abdolrezaee *et al*., 2006; Rota Nodari *et al*., 2010). To describe the various therapeutic actions/functions of transplanted NPCs *in vivo*, we have recently proposed the concept of 'therapeutic plasticity' (Martino and Pluchino, 2006).

The primary aim of this study was to provide preclinical proof-of-concept of the therapeutic plasticity of somatic mouse NPCs after their focal implantation in the contused spinal cord. We adopted an extremely severe thoracic contusion spinal cord injury model, employed two different cell doses and two time points of treatment, subacute or early chronic after the injury, and analysed locomotor functions and relevant secondary pathological events in the mice; cell fate of transplanted NPCs; and gene expression and inflammatory cell infiltration at the injured site.

In this study, only the subacute transplantation of NPCs led to significant locomotor recovery, which started at 2 weeks after transplantation and was still measurable 5 weeks later, at the end of follow-up. The clinical benefits provided by transplanted NPCs were even more evident in a less severe and more standardized spinal cord injury model.

All the anatomical analyses related to the NPC transplantation were carried out only in mice receiving 2 N injuries. The subacute NPC transplantation also promoted the healing of the severely injured spinal cord tissue, by preventing the accumulation of major secondary events, including the volume of injury, as well as the overall extent of demyelination and inflammatory cell infiltration.

We observed that only 10% of the transplanted NPCs found *in vivo* at 1 week after transplantation survived for up to 6 weeks following the transplant. The number and the localization of these late surviving NPCs did not differ between the different treatment groups. Late surviving NPCs substantially failed to undergo differentiation *in vivo* and accumulated in clusters at the outer boundaries of the injured tissue, in very close proximity to macrophage/microglial cells and blood vessels. The morphology of these areas, including the perivascular localization of NPCs and inflammatory cells, was highly reminiscent of the 'atypical ectopic perivascular niche-like areas' that we previously described after systemic NPC transplantation in rodents with experimental autoimmune encephalomyelitis and stroke (Pluchino *et al*., 2005, 2009*b*; Bacigaluppi *et al*., 2009). Transplanted NPCs confirmed a remarkable capacity to adapt their fate and features to the perivascular, inflammatory microenvironment *in vivo* and revealed a peculiar propensity to do this by maintaining an undifferentiated phenotype, while establishing contacts with endogenous phagocytes via connexin43-mediated cellular–junctional coupling. All this is in contrast with recent studies that have described behavioural improvement and robust neuronal or oligodendroglial differentiation of mammalian NPCs, upon either early or delayed (up to 8 weeks) transplantation into the rodent injured spinal cord (Ogawa *et al*., 2002; Karimi-Abdolrezaee *et al*., 2006), or both (Cummings *et al*., 2005). The issue of cell survival and integration (up to functional differentiation) at the level of the peri-lesion environment is in fact a critical point in spinal cord injury research, and *in vivo* settings must be carefully assessed after consideration of the type and entity of the applied injury (from moderate to extremely severe), as well as the biology of transplanted cells. Stem cells have some intrinsic potential to oscillate between different phenotypic and functional states in response to non-cell-autonomous environmental (kingdom-specific) cues (Scheres, 2007). This concept is well accepted at the level of discrete specialized cellular contexts called stem cell niches, and it is increasingly relevant if applied to equally discrete (atypical ectopic) stem cell niche-like areas that recapitulate developmental patterning mechanisms and are established after stem cell transplants (Pluchino *et al*., 2010). Nonetheless, we also found small numbers of transplanted NPCs expressing neural lineage markers *in vivo*. The majority of these NPC-derived cells were observed outside perivascular niche areas. This may fit with the concept that the interplay between local inflammatory signals influences the function—rather than the developmental fate (Rossi and Cattaneo, 2002)—of transplanted NPCs, by reprogramming their capacity to remodel the environment (Pluchino *et al*., 2010).

In our study, the focal transplantation of NPCs operated a striking regulation of gene expression in the lesioned cord environment, via a multilayered effect that led to a significant over-enrichment in inflammatory gene transcripts. These include the chemokine *Ccl2* and *Nos2*, as well as several cell adhesion molecules and cell adhesion molecule counter ligands. On the other hand, we found significant under enrichment of the macrophage-specific chemokine *Ccl3*, as well as of the major constituent of the perilesional extracellular matrix, *Cspg4,* and a single neurotrophin. This NPC-driven instruction of the environment appeared to be specifically regulated by transplanted NPCs, as it was observed also in chronically transplanted mice with spinal cord injury that did not respond to NPC transplantation. We speculate that NPCs retaining the capacity to affect the expression of several messenger RNAs *in vivo* when transplanted chronically to mice with spinal cord injury fail to regulate anatomical and functional changes because of the high level of axonal severance that this 2 N spinal cord injury model develops as early as 3 weeks after the injury.

The question therefore arises as to how small numbers of undifferentiated stem cells might have orchestrated all of this. On one hand, solid evidence exists that NPCs increase the availability of diffusible (tissue) trophic factors (Lu *et al*., 2003) and developmental stem cell regulators (Pluchino *et al*., 2005, 2009*b*) *in vivo*. On the other hand, there is emerging indication that cellular contacts (Pluchino *et al*., 2009*b*) and gap junction formation (Jaderstad *et al*., 2010) between grafted stem cells and host cells play a major role for ensuring host cell well-being. After the proof-of-concept of functional integration of grafted NPCs into Ca^{2+}-mediated host neuronal networks (Jaderstad *et al*., 2010), it can be envisioned that such coupling would permit more efficient (namely direct or transcellular) delivery of factors to promote cell survival and/or instruct pathological molecules or processes. Here we provide compelling correlative evidence that NPCs function by establishing multiple programmes of cell-to-cell communication *in vivo*, including the release of soluble factors and cellular–junctional coupling, other than through the replacement of lost/injured endogenous neural cells.

Transplanted NPCs significantly skewed the inflammatory infiltrate of the injured spinal cord segment. The focal transplantation of NPCs decreased the relative proportion of $CD11c^{+}/CD206^{-}$ classically activated (M1-like) cells among the macrophage-lineage cells infiltrating the injured cord and enhanced their expression of neuroprotective *Nos2* (Fenyk-Melody *et al*., 1998; Hall *et al*., 2004). These two effects may have acted in combination to shift the balance towards a tissue remodelling/repair (M2-like) mode *in vivo* at the injury site, thus promoting the adequate recovery from spinal cord injury-induced secondary damage, as suggested elsewhere (Kigerl *et al*., 2009; Nucera *et al*., 2011). *In vitro* co-cultures with BV-2 cells confirmed the capacity of NPCs to interfere with the responsiveness of CNS phagocytes to canonical inflammatory stimuli.

The NPC transplantation also increased the small proportion of T lymphocytes and decreased that of dendritic cells and B lymphocytes accumulating at the injury site. T lymphocytes isolated from the spinal cord of NPC-transplanted showed enhanced expression of regulatory (*Foxp3* and *CD25*) and effector/cytotoxic (*CD8*, *Fasl*, *Gzmb* and *Ifng)* transcripts. While robust evidence is available that a critical M1/M2 macrophage ratio has significant implications for CNS injury and repair (Rapalino *et al*., 1998; Alexander and Popovich, 2009; Shechter *et al*., 2009), much less is known about the role of regulatory/effector T-cell subsets in the regulation of inflammatory responses after CNS traumas (Moalem *et al*., 1999; Hauben *et al*., 2000), as most of the mechanistic studies have been performed in experimental autoimmune encephalomyelitis (Tsai *et al*., 2011).

Here we describe an experimental therapy using functionally multipotent stem cells that optimize their undifferentiated features to survive long-term within a putative inhospitable environment, while finding their way towards a perilesional inflammatory-like vascular niche. At the level of the atypical vascular niches, NPCs control innate (as well as adaptive) immune responses to regulate significant tissue healing and functional recovery after severe experimental spinal cord injury (Alexander and Popovich, 2009). Further studies investigating the NPC-orchestrated M1/M2 cell interactions with other cell types (e.g. T cells, B cells and dendritic cells), as well as the functional consequences of these (e.g. whether they tolerize antigen presenting cells/macrophages), and establishing their relevance for tissue healing, will be needed to test some of the hypotheses that our work has contributed to.

While providing significant evidence that a precise window of opportunity exists for somatic stem cell-based approaches to complex spinal cord injuries, our data represent a further piece of rationale for the future translation of NPC-based therapeutics in phase I clinical trials in humans suffering from spinal cord injuries.

Being successful in this, it is possible to envisage a future scenario in which either increasing the number of therapeutically plastic stem cells to transplant/deliver, or in a more sophisticated way, identifying, enhancing and/or customizing the individual mechanisms behind their functional potency, may realistically result in more efficacious cures for severe neurological syndromes.

Acknowledgements

The authors are grateful to Luca Bonfanti, Sabrina Ceeraz, Marianna Esposito, James Fawcett, Diego Franciotta and Michal Schwartz for critically reading and commenting on the manuscript, and to the anonymous reviewers for their comments to improve the quality of this study. We acknowledge the technical assistance of Adaoha E. Ihekwaba, Tommaso Leonardi, Luca Peruzzotti-Jametti and Giulia Tyzack.

Funding

Wings for Life (grant SE-013/09 to S.P.); Banca Agricola Popolare di Ragusa (BAPR, unrestricted grant to S.P.); European Research Council (ERC) under the ERC-StG Grant agreements (n° 260511-SEM_SEM to S.P.); (n° 243128-TIE2 + Monocytes to M.D.P.); Fondazione Berlucchi (to M.D.P.); the BMW Italy Group (BMW 2008 MART to G.M.).

Supplementary material

Supplementary material is available at *Brain* online.

References

Aharonowiz M, Einstein O, Fainstein N, Lassmann H, Reubinoff B, Ben-Hur T. Neuroprotective effect of transplanted human embryonic stem cell-derived neural precursors in an animal model of multiple sclerosis. PLoS One 2008; 3: e3145.

Alexander JK, Popovich PG. Neuroinflammation in spinal cord injury: therapeutic targets for neuroprotection and regeneration. Prog Brain Res 2009; 175: 125–37.

Bacigaluppi M, Pluchino S, Peruzzotti-Jametti L, Kilic E, Kilic U, Salani G, et al. Delayed post-ischaemic neuroprotection following systemic neural stem cell transplantation involves multiple mechanisms. Brain 2009; 132: 2239–51.

Barnabe-Heider F, Frisen J. Stem cells for spinal cord repair. Cell Stem Cell 2008; 3: 16–24.

Beck KD, Nguyen HX, Galvan MD, Salazar DL, Woodruff TM, Anderson AJ. Quantitative analysis of cellular inflammation after

traumatic spinal cord injury: evidence for a multiphasic inflammatory response in the acute to chronic environment. Brain 2010; 133: 433–47.

Cummings BJ, Uchida N, Tamaki SJ, Salazar DL, Hooshmand M, Summers R, et al. Human neural stem cells differentiate and promote locomotor recovery in spinal cord-injured mice. Proc Natl Acad Sci USA 2005; 102: 14069–74.

Donnelly DJ, Longbrake EE, Shawler TM, Kigerl KA, Lai W, Tovar CA, et al. Deficient CX3CR1 Signaling Promotes Recovery after Mouse Spinal Cord Injury by Limiting the Recruitment and Activation of Ly6Clo/iNOS+ Macrophages. J Neurosci 2011; 31: 9910–22.

Einstein O, Friedman-Levi Y, Grigoriadis N, Ben-Hur T. Transplanted neural precursors enhance host brain-derived myelin regeneration. J Neurosci 2009; 29: 15694–702.

Engstrom CM, Demers D, Dooner M, McAuliffe C, Benoit BO, Stencel K, et al. A method for clonal analysis of epidermal growth factor-responsive neural progenitors. J Neurosci Methods 2002; 117: 111–21.

Fenyk-Melody JE, Garrison AE, Brunnert SR, Weidner JR, Shen F, Shelton BA, et al. Experimental autoimmune encephalomyelitis is exacerbated in mice lacking the NOS2 gene. J Immunol 1998; 160: 2940–6.

Follenzi A, Ailles LE, Bakovic S, Geuna M, Naldini L. Gene transfer by lentiviral vectors is limited by nuclear translocation and rescued by HIV-1 pol sequences. Nat Genet 2000; 25: 217–22.

Hall ED, Detloff MR, Johnson K, Kupina NC. Peroxynitrite-mediated protein nitration and lipid peroxidation in a mouse model of traumatic brain injury. J Neurotrauma 2004; 21: 9–20.

Hauben E, Nevo U, Yoles E, Moalem G, Agranov E, Mor F, et al. Autoimmune T cells as potential neuroprotective therapy for spinal cord injury. Lancet 2000; 355: 286–7.

Hoffmann JA, Kafatos FC, Janeway CA, Ezekowitz RA. Phylogenetic perspectives in innate immunity. Science 1999; 284: 1313–8.

Jaderstad J, Jaderstad LM, Li J, Chintawar S, Salto C, Pandolfo M, et al. Communication via gap junctions underlies early functional and beneficial interactions between grafted neural stem cells and the host. Proc Natl Acad Sci USA 2010; 107: 5184–9.

Karimi-Abdolrezaee S, Eftekharpour E, Wang J, Morshead CM, Fehlings MG. Delayed transplantation of adult neural precursor cells promotes remyelination and functional neurological recovery after spinal cord injury. J Neurosci 2006; 26: 3377–89.

Kigerl KA, Gensel JC, Ankeny DP, Alexander JK, Donnelly DJ, Popovich PG. Identification of two distinct macrophage subsets with divergent effects causing either neurotoxicity or regeneration in the injured mouse spinal cord. J Neurosci 2009; 29: 13435–44.

Lindvall O, Kokaia Z. Stem cells in human neurodegenerative disorders–time for clinical translation? J Clin Invest 2010; 120: 29–40.

Lu P, Jones LL, Snyder EY, Tuszynski MH. Neural stem cells constitutively secrete neurotrophic factors and promote extensive host axonal growth after spinal cord injury. Exp Neurol 2003; 181: 115–29.

Martino G, Pluchino S. The therapeutic potential of neural stem cells. Nat Rev Neurosci 2006; 7: 395–406.

Moalem G, Leibowitz-Amit R, Yoles E, Mor F, Cohen IR, Schwartz M. Autoimmune T cells protect neurons from secondary degeneration after central nervous system axotomy. Nat Med 1999; 5: 49–55.

Moon L, Bunge MB. From animal models to humans: strategies for promoting CNS axon regeneration and recovery of limb function after spinal cord injury. J Neurol Phys Ther 2005; 29: 55–69.

Nielson JL, Sears-Kraxberger I, Strong MK, Wong JK, Willenberg R, Steward O. Unexpected survival of neurons of origin of the pyramidal tract after spinal cord injury. J Neurosci 2010; 30: 11516–28.

Nishi RA, Liu H, Chu Y, Hamamura M, Su MY, Nalcioglu O, et al. Behavioral, histological, and ex vivo magnetic resonance imaging assessment of graded contusion spinal cord injury in mice. J Neurotrauma 2007; 24: 674–89.

Nucera S, Biziato D, De Palma M. The interplay between macrophages and angiogenesis in development, tissue injury and regeneration. Int J Dev Biol 2011; 55: 495–503.

Ogawa Y, Sawamoto K, Miyata T, Miyao S, Watanabe M, Nakamura M, et al. Transplantation of in vitro-expanded fetal neural progenitor cells results in neurogenesis and functional recovery after spinal cord contusion injury in adult rats. J Neurosci Res 2002; 69: 925–33.

Onose G, Anghelescu A, Muresanu DF, Padure L, Haras MA, Chendreanu CO, et al. A review of published reports on neuroprotection in spinal cord injury. Spinal Cord 2009; 47: 716–26.

Pluchino S, Cusimano M, Bacigaluppi M, Martino G. Remodelling the injured CNS through the establishment of atypical ectopic perivascular neural stem cell niches. Arch Ital Biol 2010; 148: 173–83.

Pluchino S, Gritti A, Blezer E, Amadio S, Brambilla E, Borsellino G, et al. Human neural stem cells ameliorate autoimmune encephalomyelitis in non-human primates. Ann Neurol 2009a; 66: 343–54.

Pluchino S, Muzio L, Imitola J, Deleidi M, Alfaro-Cervello C, Salani G, et al. Persistent inflammation alters the function of the endogenous brain stem cell compartment. Brain 2008; 131: 2564–78.

Pluchino S, Quattrini A, Brambilla E, Gritti A, Salani G, Dina G, et al. Injection of adult neurospheres induces recovery in a chronic model of multiple sclerosis. Nature 2003; 422: 688–94.

Pluchino S, Zanotti L, Brambilla E, Rovere-Querini P, Capobianco A, Alfaro-Cervello C, et al. Immune regulatory neural stem/precursor cells protect from central nervous system autoimmunity by restraining dendritic cell function. PLoS One 2009b; 4: e5959.

Pluchino S, Zanotti L, Rossi B, Brambilla E, Ottoboni L, Salani G, et al. Neurosphere-derived multipotent precursors promote neuroprotection by an immunomodulatory mechanism. Nature 2005; 436: 266–71.

Pucci F, Venneri MA, Biziato D, Nonis A, Moi D, Sica A, et al. A distinguishing gene signature shared by tumor-infiltrating Tie2-expressing monocytes, blood "resident" monocytes, and embryonic macrophages suggests common functions and developmental relationships. Blood 2009; 114: 901–14.

Rapalino O, Lazarov-Spiegler O, Agranov E, Velan GJ, Yoles E, Fraidakis M, et al. Implantation of stimulated homologous macrophages results in partial recovery of paraplegic rats. Nat Med 1998; 4: 814–21.

Rossi F, Cattaneo E. Opinion: neural stem cell therapy for neurological diseases: dreams and reality. Nat Rev Neurosci 2002; 3: 401–9.

Rota Nodari L, Ferrari D, Giani F, Bossi M, Rodriguez-Menendez V, Tredici G, et al. Long-term survival of human neural stem cells in the ischemic rat brain upon transient immunosuppression. PLoS One 2010; 5: e14035.

Scheres B. Stem-cell niches: nursery rhymes across kingdoms. Nat Rev Mol Cell Biol 2007; 8: 345–54.

Schwab JM, Brechtel K, Mueller CA, Failli V, Kaps HP, Tuli SK, et al. Experimental strategies to promote spinal cord regeneration–an integrative perspective. Prog Neurobiol 2006; 78: 91–116.

Shechter R, London A, Varol C, Raposo C, Cusimano M, Yovel G, et al. Infiltrating blood-derived macrophages are vital cells playing an anti-inflammatory role in recovery from spinal cord injury in mice. PLoS Med 2009; 6: e1000113.

Tsai S, Clemente-Casares X, Santamaria P. CD8(+) Tregs in autoimmunity: learning "self"-control from experience. Cell Mol Life Sci 2011; 68: 3781–95.